Metabolic profiling of Pseudomonas aeruginosa demonstrates that the anti-sigma factor MucA modulates osmotic stress tolerance

Metabolic profiling of *Pseudomonas aeruginosa* demonstrates that the anti-sigma factor MucA modulates osmotic stress tolerance

Volker Behrends[1,2*], Ben Ryall[2], Xinzhu Wang[1], Jacob G. Bundy[1], Huw D. Williams[2]

1: Biomolecular Medicine, Department of Surgery and Cancer, Faculty of Medicine, Imperial College London, London SW7 2AZ, UK
2: Department of Life Sciences, Faculty of Natural Science, Imperial College London, London SW7 2AZ, UK

*Corresponding author.
Email: volker.behrends05@imperial.ac.uk
Telephone: +44 20 75943202

Summary

Metabolic footprinting has shown enormous potential as a phenotyping tool and we are interested in applying it to understand the physiology of the opportunistic pathogen *Pseudomonas aeruginosa* during its chronic infection of the lungs of cystic fibrosis patients. The selection pressures of surviving in the CF lung environment lead to genetic adaptations of the bacterium. A common adaptation is mutation of the *mucA* gene, resulting in a loss-of-function mutation to the anti-sigma factor MucA, which leads to a mucoid phenotype as a consequence of the overproduction of the extracellular polysaccharide alginate. However, apart from the mucoid phenotype little is known about the overall metabolic and physiological changes caused by *mucA* mutation. We investigated the pleiotropic metabolic effects of this mutation using time-resolved metabolic footprinting (extracellular metabolomics), and found changes in various metabolites associated with osmotic tolerance, including glycine-betaine, trehalose and glutamate. Physiological experiments confirmed that the isogenic *mucA22* mutant is less resistant to osmotic stress than the parental PA01 wild-type strain, but only in the stationary phase of growth. Quantitative comparison of the endometabolome of the cells showed differences in the accumulation of osmoprotective metabolites by the wild-type and *mucA22* mutant strains, suggesting a switch in osmo-protectant preference from glycine-betaine to trehalose.

Introduction

The opportunistic pathogen *Pseudomonas aeruginosa* is associated with infection of immuno-compromised patients such as those with cystic fibrosis (CF).[1] One hallmark of long-term *P. aeruginosa* CF infection is the emergence of an alginate-overproducing, mucoid phenotype.[2] Understanding the consequences of the switch to alginate overproduction is crucial to further understanding of how *P. aeruginosa* is able to achieve such persistent and problematic infections. Mucoidy is commonly associated with worsening of prognosis and accelerated loss of lung function.[1,3] The mechanisms controlling conversion to mucoidy and the genes and proteins involved in alginate synthesis have been an active field of research for more than four decades, and excellent reviews exist.[3,4] Briefly, alginate is synthesised in a pathway beginning at fructose-6-phosphate, which is converted intra-cellularly to GDP-mannuronic acid, the principal building block of alginate. GDP-mannuronic acid is then polymerised and exported to the periplasm. Some residues are then epimerised to the C5-epimer guluronic acid and some of the remaining mannuronic acid residues are acetylated prior to transport of the finished alginate across the outer membrane.[3]

The exact environmental function for alginate apart from the apparent advantage in long-term CF infections is still under investigation. Alginate has been proposed to protect against phagocytosis[5] and oxygen radicals.[6] Induction by low oxygen concentrations in the CF lung has been suggested,[7] but alginate was also shown to be upregulated in response to increased oxygen concentration.[8,9] Further, it could be involved in CF end-stage biofilm formation, but is not a major component of non-mucoid *P. aeruginosa* biofilms.[3] The genes for alginate synthesis are arranged in the *algD* operon (PA3540-PA3551) under the control of the alternative sigma factors AlgU (σ^{22}, also referred to as AlgT)[10,11] and RpoN (σ^{54})[12]. The *algU* gene is the first gene of the *algU mucABCD* operon and the products of the *mucABCD* genes play a role in regulating the activity of AlgU. The MucA protein is an anti-sigma factor specific for AlgU. MucA along with MucB sequesters AlgU at the inner surface of the cytoplasmic membrane preventing it from forming RNA polymerase

holoenzyme complex and hence directing the transcription of its target genes.[13-15] The most common route to mucoidy in *P. aeruginosa* isolates recovered from long-term CF lung infection is via mutations in the *mucA* gene that prevent the anti-sigma factor from sequestering AlgU leaving it free to direct transcription of its target genes, which include the alginate biosynthetic genes located in the *algD* operon.[16] So loss of AlgU regulation via *mucA* mutation results in alginate overproduction. The most common mutation, referred to as *muc-22 or mucA22*,[17] is a single base-pair deletion resulting in a truncated, dysfunctional MucA protein. The *alg* genes are not normally expressed in the wild-type, and presumably constitutive alginate expression in wild-type cells would represent a poor use of metabolic resources. AlgU-responsive promoter sequences were found for at least 35 genes, among them many stress-induced genes like those encoding the heat shock proteins DnaK, DnaJ and GrpE.[18,19] Additionally, the *mucA* mutation was suggested to have several effects on virulence factors including increased cyanide production on plate culture,[20] reduced T3SS expression,[21] and could also have an effect on twitching motility[22] via increased levels of AlgU.

A major asset of 'omics' approaches is their inherent ability to generate *a posteriori* hypotheses based on systematic data collection.[23,24] Metabolomics approaches have shown great promise in that area, often uncovering unexpected effects of mutations.[25,26] Metabolism is downstream of the genome or the proteome, and so provides information at the most functional level,[27,28] including complex integrated phenotypes that do not depend simply on single genes and thus cannot be easily predicted from genome sequences alone. Metabolic footprinting is the study of the extracellular metabolite pools and thus circumvents the problematic question of bacterial sampling and quenching.[29] Allen *et al*. used metabolic footprinting to distinguish between several yeast mutants.[30] In a similar study, Kaderbhai *et al.* were able to discriminate several *E. coli* strains harbouring mutations in tryptophan metabolism.[31] Behrends *et al.* monitored the time-dependent utilisation of compounds from the medium and used the data for characterisation of differences between *P. aeruginosa* and *Burkholderia cepacia* complex wild-type strains.[32]

Here we used time-resolved metabolic footprinting (TReF)[32] to investigate the pleiotropic effects of the *mucA* mutation on *P. aeruginosa* metabolism. From the results, we proposed the novel hypothesis that MucA plays a role in osmotic tolerance, and then carried out physiological tests to demonstrate that a functional MucA protein is required for normal osmotic tolerance in *P. aeruginosa*.

Methods

Bacteria and culturing: The strains used were *Pseudomonas aeruginosa* PA01 and its isogenic *mucA22* mutant (see below). Starter cultures were set up by inoculating single colonies into 5 ml of Luria Bertani (LB) medium (10 g/L tryptone, 5 g yeast extract, 5 g NaCl) or synthetic cystic fibrosis medium (SCFM), a complex defined medium designed to model nutrient status in sputum.[33] The cultures were grown overnight at 37°C, shaking at 150 rpm. These cultures were used to inoculate 20 ml of LB or SCFM in 250 ml conical flasks and then grown for 24 h at 37°C shaking at 150 rpm.

Construction of *mucA22* mutant: A *mucA22* mutant was constructed in the *P. aeruginosa* PAO1 background by inserting a 1 kb fragment containing the *mucA22* mutation from PA0578 genomic DNA (mucoid, *mucA22 P. aeruginosa* strain[34]). Primers for amplification were 5'-GCAATCGACAAAGCTCTGCAG-3' and 5'-CATCAGGCTGCCAAGCAAAAG-3'. Fragments were cloned in pGEM-T Easy, checked by sequencing and inserted into the NotI site of the positive selection suicide vector pJQ200KS.[35] The resulting plasmid pBR002 was introduced into *P. aeruginosa* by conjugation with *E. coli* S17.1. Single crossovers were selected for with gentamicin, double crossovers were selected via the *sacB* – sucrose system on LB + 5% sucrose plates. Finally, the presence of the correct mutation in the *P. aeruginosa* genome was verified by sequencing of a PCR amplicon of the *mucA* gene from the transconjugant.

Sampling: Supernatants: Sampling and sample preparation of supernatants was performed as described before.[32] Briefly, 1 ml of supernatant was sampled at 12 time points throughout growth from all cultures. 0.1 ml was diluted 1:10 for cell density (OD_{600}) measurements. The remainder was centrifuged (16000 x *g*, RT) and 0.75 ml of the supernatant was mixed with 0.2 ml NMR buffer (25 mM sodium azide, 0.25 M phosphate buffer pH 7, and 5 mM sodium 3-trimethylsilyl-2,2,3,3-$^2H_4$-propionate (TSP), in ^2H_2O). The ^2H_2O provided a field frequency lock for the spectrometer and the TSP served as an internal chemical shift reference. Extracts: The culture was centrifuged (10 min, 3600 *xg*, RT). The pellets were washed with 5 ml quarter strength

Ringer's solution, centrifuged again and resuspended in 5 ml of previously cooled (-20 °C) methanol-water 75:25 % (v/v). The cells were sonicated for 10 min and the extracts dried following removal of cell debris by centrifugation (5 min). The residues were resuspended in 0.6 ml 0.1 M phosphate, pH 7.0, 90 % $^{2}H_{2}O$ with 1 mM TSP.

Physiological experiments: Osmotic tolerance was assessed by growing three replicates of PA01 and the *mucA22* mutant in LB supplemented with different NaCl concentration (0, 0.1M, 0.2M, 0.3M, 0.4M, 0.5M. 0.6M, 0.7M and 0.8M). The endo- and exometabolome was quantified after 24h. Additionally, metabolite uptake and excretion were characterised over the course of growth for the 0M and 0.4M concentrations. To examine the variability of the strains' OD readings, both strains were grown in 24-well plates containing LB supplemented with 0M, 0.2M, 0.5M and 0.8M NaCl.

^{1}H NMR spectroscopy: Spectra were acquired on a Bruker Avance DRX600 NMR spectrometer (Bruker BioSpin, Rheinstetten, Germany), with a magnetic field strength of 14.1 T and resulting ^{1}H resonance frequency of 600 MHz, equipped with a 3 mm inverse flow probe. Samples were introduced using a Gilson flow-injection autosampler. Spectra were acquired following the approach given by Beckonert *et al.*[36] Briefly, a one-dimensional NOESY pulse sequence was used for water suppression; data were acquired into 32 K data points over a spectral width of 12 kHz. Spectra were acquired with 8 dummy scans and 128 scans per sample, and an additional longitudinal relaxation recovery delay of 2 s per scan, giving a total recycle time of 3.5 s.

Spectral processing and data analysis: Spectra were processed in iNMR 2.5 (Nucleomatica, Molfetta, Italy). Free induction decays were multiplied by an exponential apodization function equivalent to 0.5 Hz line broadening, followed by Fourier transformation. Spectra were manually phased and automated first order baseline correction was applied. Spectral data between –0.5 and 10 ppm were then imported into Matlab 2008b (MathWorks, Cambridge, UK) and normalized to the integral of the TSP signal for supernatants and the total spectral area in case of the extracts.

Modelling for TReF and pattern recognition analysis

Principal Component Analysis (PCA) and orthogonal Partial Least Squares-Discriminant Analysis (oPLS-DA)[37] were carried out using in-house code[38] on

full resolution spectra and sigmoid parameters, respectively. Sigmoid modelling of resonance evolution and hierarchical PCA (H-PCA)[39] on the resulting parameters were carried out as described before.[32] Briefly, spectral regions containing ‘real’ peaks were defined by visual inspection and the evolution of the integrals over the course of growth was fitted with sigmoid equations. The equation returns four sigmoid parameters, two of which (half-life and slope) were used to produce ‘uptake plots’ and three (half-life, slope and amplitude) as inputs for H-PCA.

Results

NMR analysis of *P. aeruginosa* PA01 and *mucA22* culture supernatants reveals multiple differences

Previous studies have suggested that 'omics' technologies and metabolomics in particular[28] could act as hypothesis generators[23,24] by uncovering unexpected phenotypes. We compared the supernatants of rich medium cultures of the *P. aeruginosa* wild-type PA01 and its isogenic, mucoid *mucA22* mutant using metabolic footprinting. Figure 1 shows the spectral representation of an oPLS-DA of PA01 and *mucA22* supernatants sampled after 24 h of growth. The analysis indicated that the levels of several compounds such as valine, methionine, glycine-betaine, trehalose, and an unidentified putative sugar resonance at 5.26 ppm were highly discriminatory between the wild type and *mucA22* mutant after 24 h. Compound levels clearly differed over the course of growth and relative concentration changes of these compounds are shown in Figure 2. Valine levels exhibited transient excretion followed by uptake, but the kinetics for the *mucA22* mutant were clearly delayed (Figure 2 A). Both methionine and the unknown compound with a resonance at 5.26 ppm were constantly excreted by the *mucA*22 mutant only (Figure 2 B and E). In contrast, trehalose was taken up quicker by the *mucA* mutant strain (Figure 2 D). Interestingly, glycine-betaine exhibited a transient-excretion-followed-by-uptake phenotype for PA01, but remained relatively unchanged in the *mucA* supernatants (Figure 2 C). Choline levels showed a substantial transient increase in the supernatants of wild-type strains only (Figure 2 F), but there were no strain differences by the end of the 24 h incubation. Trehalose and glycine-betaine have previously been identified as contributing to the osmotic tolerance of *P. aeruginosa*[40] and choline is a precursor of glycine-betaine.[41] These findings led us to hypothesise that wildtype and its isogenic *mucA22* mutant strains might show differences in their tolerance to osmotic stress.

A functional *mucA* gene product is required for full osmotic tolerance of *P. aeruginosa* in stationary phase

As an initial test, we grew both *P. aeruginosa* PA01 and the *mucA22* mutant in LB medium supplemented with 0.4M NaCl. Though growth rates of both

wild-type and mutant were reduced compared to unsupplemented media, there were no *mucA*-related effects on growth during exponential phase. However, following the onset of stationary phase, growth of the mutant levelled off while the wild-type grew to optical densities similar to those reached by both the wild-type and the mutant in the absence of extra salt (Figure 3 A and B). To investigate the concentration dependence of this phenotype, we grew both strains in LB supplemented with a range of salt concentrations (Figure 3 C). Although the growth curves were identical in standard unsupplemented medium, the *mucA22* mutant always reached lower optical densities in stationary phase than the wild-type under salt-stress conditions. This was caused by a decrease in viable cell number, as verified by counting colony-forming units in cultures grown to stationary phase across all salt concentrations (Figure 3 D). While consistent significant differences were seen between the mutant and the wild-type, the *mucA22* mutant replicate cultures in particular had higher variance in their final stationary phase optical density after 24 h growth than the wild-type cultures (see error bars in Figure 3 C). We grew both strains at higher replication (n = 72) at four different salt concentrations (0, 0.2, 0.5 and 0.8M added NaCl) to better characterize the variation. There was some variation across all investigated salt concentrations (Figure 3 E). However, the stationary phase optical density was significantly reduced for the *mucA22* strain at all salt concentrations above zero (two-way ANOVA, Fisher's LSD test, $P < 0.001$ at all concentrations). This clearly shows that the *mucA22* mutant is less resistant to osmotic stress and that a functional MucA protein is required for normal osmotic tolerance in stationary phase but not during exponential growth. The effect is not peculiar to a single medium (LB), as we obtained similar results using synthetic cystic fibrosis sputum medium[33], designed to mimic nutritional conditions in the CF lung (data not shown). Neither was the effect NaCl-specific, as cells stressed with 0.5M of the non-metabolizable sugar sucrose showed similar results (data not shown).

Exo- and endometabolome analysis reveals concentration dependence of osmoprotectants

In order to identify the compounds responsible for osmotolerance, the endo- and exo-metabolomes of *P. aeruginosa* PA01 and its *mucA22* mutants were analysed after 24 h of growth in LB supplemented with different salt concentrations. For the exo-metabolome, only glycine-betaine was positively osmo-responsive, i.e. uptake increased in response to higher salt concentrations (not shown). Additionally, spectral analysis of the supernatants also detected two closely related compounds apparently excreted in response to osmotic stress by the *mucA22* mutant strain (Figure 3 F). Both compounds only differed in one visible (non-overlapped) resonance, a doublet at 5.25 ppm, but were otherwise identical. While the compounds were not detected universally, i.e. they appeared only in some biological replicates, it appeared in both LB and SCFM media and in response to NaCl as well as sucrose. A heteronuclear single quantum coherence spectrum was acquired, and ^{1}H and ^{13}C chemical shifts pairs were found to be ($\delta^{1}H$/ $\delta^{13}C$ (ppm)): 5.82/110.67, 5.78/110.67, 5.26/96.31, 5.25/95.04, 5.23/96.55, 5.19/102.66, 5.12/102.99, 4.95/96.58. Both carbon as well as hydrogen shifts are consistent with the unknown compounds being oligosaccharides, the nature of which is discussed below.

For the endo-metabolome, several compounds were found to increase in response to elevated salt concentrations. From the spectra, N-acetylglutaminylglutamine amide (NAGGN,[42] resonances: 2.08s, 2.13m, 2.40m, 4.30dd, 4.34dd), trehalose (3.46t, 3.65dd, 3.83d, 3.86m, 3.88t, 5.20d), glycine-betaine (3.27s, 3.90s) and glutamate (2.07m, 2.36m, 3.74t) were identified (Figure 4A). Glycine-betaine conjugates are a known osmo-protectant for many organisms, while an osmo-protective function has been attributed to NAGGN, glutamate and trehalose in *P. aeruginosa*.[40] Quantification of the relative intracellular concentration changes revealed that while NAGGN, glutamate, trehalose and glycine-betaine all increased in response to NaCl (Figure 4 B-E), the levels of all of these compounds were lower in the *mucA22* mutant compared to wild-type at the highest NaCl concentrations: the mutant strain reached maximum levels of osmo-protectants around 0.6M NaCl and exhibited reduced levels of all four compounds for higher concentrations. At lower NaCl concentrations, the wild-

type levels were higher for glycine-betaine, but not significantly changed for NAGGN or glutamate. The effects of *mucA* status on osmo-protectant responses were particularly clear for trehalose, where the wild-type showed a clear dose-response increasing up to 0.8M NaCl, but the concentrations in the mutant reached a maximum at 0.4M NaCl and decreased after that (Figure 4 E). At lower salt concentrations, however, trehalose levels were higher in the *mucA22* mutant.

Footprinting analysis reveals differential effects of salt stress on the metabolism of the *mucA22* mutant

In an attempt to elucidate the effects of osmotic stress on general cellular physiology, we grew the wild-type and mutant strains in normal and elevated salt (0.4M NaCl) LB medium and analysed the media composition at various time-points. PCA of the data set clearly showed the effects of NaCl stress on exometabolome profiles, and hinted at differences between stressed and unstressed cultures, but the variance introduced by overall growth effects dominated the results, i.e. separation along PC 1 was basically a depiction general signal decrease from the medium due to growth (Figure 5 A). The treatment difference was clearest at intermediate times, and converged after 24h, suggesting that single time-point analysis might have been inconclusive on this data set.

In order to summarize all the metabolic data across the course of growth in a principled way as opposed to *ad hoc* selection of individual time points, we used time-resolved metabolic footprinting (TReF), a combined sampling and data analysis approach, which allows us to systematically examine metabolite utilisation and excretion. The approach is based on fitting the changes in the relative intensities of the NMR resonances over time to sigmoid equations. Summarising the changes over time in four parameters. One parameter (the amplitude) is a direct measure of the overall concentration change, and two others (the t_{50} and the width) are measures of the time and speed of uptake or secretion and can be used for a graphical representation of uptake (Figure 5 C-F, for more details see ref[32]).

Additionally, the individual fitted parameters of the sigmoid equation can be analysed using a hierarchical principal components approach.[39] Firstly, three separate PCA models were calculated for the fitted sigmoid parameters, i.e. the amplitude, half-life and width (speed of the concentration changes). The scores of these three PCA models were then concatenated and used as inputs for a second-level PCA. This H-PCA very clearly showed unequivocal genotype-specific metabolic responses to osmotic stress (Figure 5 B). Investigation of the loadings pointed to several compounds responsible for these separations. (Figure 5 C-F) compares the uptake characteristics for five compounds, the amino acids glutamate, valine and pyroglutamate, as well as trehalose and glycine-betaine, over the course of growth. Osmotic stress had a profound effect on the metabolite utilisation behaviour of both strains. Valine was transiently excreted during the course of growth in standard LB medium (Figure 2 A), but was taken up in a sigmoid fashion by both strains when osmotically stressed. Interestingly, differences between the wild-type and the *mucA22* mutant were particularly clear for known osmoprotectants (Figure 5 C-F). When under salt stress, both strains take up glycine-betaine in a sigmoid fashion. However, the *mucA22* mutant takes up glycine-betaine at a later stage of growth than its wild-type counterpart. Further, glutamate is also taken up later by the mutant than the wild-type strain. Trehalose is taken up quicker and to a greater extent by the *mucA22* mutant in unstressed conditions (Figure 5 C and E and Figure 2 D). Under osmotic stress, it is not utilised to a great degree by the wild-type, but is taken up, albeit at a late phase of growth, by the *mucA22* mutant.

Discussion

Previous studies utilising metabolic profiling for questions regarding microorganisms have shown that the approach can be useful for finding biomarkers of clinical strains[43] or distinguishing between different mutants.[30,31] A major strength of unbiased profiling approaches should be the potential to generate testable biological hypotheses.[23] However, it is frequently the case that these hypotheses are not actually tested, and the results therefore remain speculative. In the present study, we utilised untargeted NMR-based metabolic footprinting to investigate differences between *P. aeruginosa* PA01 and its isogenic *mucA22* mutant, which is known to over-produce the exopolysaccharide alginate, and then tested and validated a novel hypothesis generated solely on the basis of the metabolic profiling data. While both strains grew to similar optical densities in the rich medium LB, there were several differences in the exometabolome profiles for the two strains. As many of the changes pointed towards alterations in the strains' osmotic stress response, this was investigated in more detail. It was shown that the *mucA22* mutant was clearly more susceptible to osmotic stress than the wild-type. The effect was highly significant for all tested NaCl concentration other than from unsupplemented LB (which contains 0.089M NaCl).

There is an established link between alginate, the sigma factor AlgU and osmotic stress in pseudomonads. Alginate production is a common stress-response phenotype for *P. syringae*[44] including the response to osmotic stress; in *P. fluorescens* CHA0, AlgU was found to be important for osmotic stress resistance during logarithmic growth.[45] Further, in *P. aeruginosa betT*, a choline transporter in the glycine-betaine biosynthesis locus (*bet*), is under the control of AlgU[18] and it has been suggested that AlgW, the MucA cleaving protease, is activated upon sensing high osmolarity in the medium.[46] In contrast, however, no alginate was produced in osmotically stressed wild-type cultures of *P. aeruginosa*, even though transcription of *algD*, the key regulatory enzymes of alginate synthesis[47] was upregulated.[48] Micro-array data suggests that while a*lgU* and *mucA* and *mucB* were upregulated following osmotic shock in *P. aeruginosa* PA01, this wasn't the case under chronic osmotic stress.[49] The *mucA22* mutation, one of the most common

mutations found in clinical isolates, leads to a loss of a functional MucA protein with the consequent failure to sequester the sigma factor AlgU to the cytoplasmic membrane, freeing the sigma factor to direct transcription of its target genes. The data presented here convincingly demonstrates that *mucA22* mutation results in a marked increase in susceptibility of stationary phase cultures to osmotic stress. This data is in apparent contradiction to the finding that *algD* and *algU* are **upregulated** in response to osmotic stress. As *algU* is in an operon with *mucA*, the fact that *algU* is induced by osmotic stress, but a *mucA22* mutation (that will increase available amounts of AlgU within the cell) leads to osmotic sensitivity is puzzling. One hypothesis is that sigma factor competition/antagonism is occurring here between AlgU and the σ^S/RpoS of *P. aeruginosa* leading to a failure to induce RpoS regulated pathways, including stationary phase osmotic stress resistance.[50-53] We are currently investigating this idea.

The relatively high NaCl concentrations encountered in the CF lung[54] mean that colonising bacteria are likely to encounter osmotic stress.[49] The effect of the *mucA* mutation on osmotic stress sensitivity is restricted to stationary phase and this contrasts with previously described osmotic stress mutants such as a disruption of synthesis of the osmoprotectant glycine-betaine, which leads to growth impairment under osmotic stress.[49] This is an interesting finding as it links the effects of a *mucA* mutation to stationary phase physiology and while the acquisition of osmotic stress sensitivity might not be beneficial, perhaps some other, as yet undiscovered, stationary phase phenotype(s) linked to *mucA* mutation plays a role in survival *in vivo*. After initial infection of the lung *P. aeruginosa* is likely to find itself mostly in a non-growing or slow growing state, perhaps in a biofilm-like structure, and resembling the stationary phase of the planktonic growth cycle.

In this study, we concentrated on the effects of the *mucA* mutation on the metabolic aspects of the osmotic stress response and decided to look at the changes of the endo- and exometabolome in more detail. NMR spectroscopy is especially suitable for this kind of analysis as it is non-selective and the relatively low sensitivity of NMR spectroscopy is not an issue, because

osmolytes need to be present in comparatively high concentrations to have an effect. As a consequence, NMR spectroscopy has been successfully applied to the study of environmental stresses like osmotic[55,56] or metal-induced[57] stress for a variety of organisms. In the present study, we found four major compounds, NAGGN, glutamate, trehalose and glycine-betaine, had increased levels in the endo-metabolome at higher salt concentrations. This was largely in accordance with the findings of D'Souza-Ault and colleagues[40] who identified the same compounds using ^{13}C NMR. Interestingly, however, they found that addition of glycine-betaine to a minimal medium prevented accumulation of trehalose in PA01 cells. Conversely, our data indicate that trehalose accumulation is dependent on extracellular NaCl concentration despite glycine-betaine being present in (and taken up from) LB.

MucA-dependent uptake of several compounds was affected by osmotic stress, particularly trehalose and glycine-betaine. In unstressed cultures, both strains took up trehalose, and glycine-betaine was taken up during stationary phase by the wild-type but not by the *mucA22* mutant. In contrast, at elevated NaCl levels only the *mucA22* mutants took up trehalose; both took up glycine-betaine, although the wild-type used up glycine-betaine much earlier during growth.

In line with the results for the endo-metabolome analysis, the footprinting analysis thus implied that, while glycine-betaine still has a function as osmo-protectant, trehalose is of more significance in the *mucA* mutants. At physiological salt concentrations, the *mucA* mutant exhibited a reduced glycine-betaine uptake and an increased trehalose uptake. This is consistent with an increased need for flux through glycolysis because of the biosynthetic demands of alginate production, as GDP-mannuronic acid is synthesised from the glycolytic intermediate fructose-6-phosphate.[3] However, the relative concentrations of the intracellular compounds were comparatively variable, so further experiments need to be conducted to confirm these results.

A separate finding was the excretion of two unknown metabolites, putative oligosaccharides. The compounds were only found in the supernatant of

some *mucA22* replicates and appeared only in response to osmotic stress. It is therefore likely that they were the result of a secondary mutation in the mutants that was selected for by osmotic stress. While the nature of these compounds was not fully resolved, the resonances cannot simply be from intact alginate.[58] Published spectral data, however, suggest the excretion of the unknown compounds might be the result of mutations in the alginate biosynthesis pathway. Mutation in one of the essential genes involved in alginate biosynthesis results in lysis of the proto-alginate by alginate lyase, AlgL.[3] AlgG epimerises mannuronic to guluronic acid; the proton NMR spectrum of *algG* mutant supernatant shows striking similarities to our observed results.[59] In particular, the *algG* spectrum contains a doublet resonance at 5.81 ppm, multiple unresolved resonances around 5.20 ppm, and a broad singlet at 4.95 ppm. While these match the resonances of the unknown compound found in this study, we also observed resonances at 5.77 and 5.12 ppm, suggesting that the compound might contain guluronic acids. The spectrum of (mature) *P. aeruginosa* alginate treated with AlgL from *Azotobacter vinelandii*[60] is also similar, but not identical to the spectra observed here. Most notably, the relative resonance intensities are different and Ertesvag *et al*. record three doublet resonances around 5.81 ppm whereas only two were detected in this study. The alginate synthesis pathway is complex, with over a dozen enzymes, and so it is likely that mutations in the pathway could lead to a range of related saccharide compounds. We suggest the metabolites found in the high osmotic stress supernatants of the *mucA22* mutant strain were the result of two separate (secondary) mutations in the *alg* genes that modify proto-alginate subsequent to epimerisation by AlgG. Full verification and characterization of these mutations is beyond the scope of our current study, but it would be interesting in the future to determine the exact nature and frequency of this mutation.

Conclusion

The mucoid phenotype of *P. aeruginosa* has been intensely studied for decades; still this study – to our knowledge – represents the first linking of the *mucA* mutation to reduced osmotic stress tolerance. Therefore, this study has established that TReF is an effective hypothesis-generating tool and may

have widespread applications in uncovering the functions of unknown genes in bacteria and refining and extending our views of the role of well established genes in bacteria.

Acknowledgements

VB was funded for a PhD studentship by Imperial College London. Work in HDW's laboratory was funded by the BBSRC. The authors thank Dr Olaf Beckonert for technical assistance with NMR spectroscopy, and Prof Jeremy Nicholson for development and provision of software, support and advice.

References

1. J. B. Lyczak, C. L. Cannon and G. B. Pier, *Clin. Microbiol. Rev.*, 2002, **15**, 194-222.
2. J. Govan and V. Deretic, *Microbiol. Rev.*, 1996, **60**, 539-574.
3. D. M. Ramsey and D. J. Wozniak, *Mol. Microbiol.*, 2005, **56**, 309-322.
4. P. Gacesa, *Microbiology (Reading, U. K.)*, 1998, **144 (Pt 5)**, 1133-1143.
5. S. Schwarzmann and J. Boring, *Infect. Immun.*, 1971, **3**, 762-767.
6. K. Mathee, O. Ciofu, C. Sternberg, P. W. Lindum, J. I. Campbell, P. Jensen, A. H. Johnsen, M. Givskov, D. E. Ohman, S. Molin, N. Høiby and A. Kharazmi, *Microbiology (Reading, U. K.)*, 1999, **145 (Pt 6)**, 1349-1357.

7. D. Worlitzsch, R. Tarran, M. Ulrich, U. Schwab, A. Cekici, K. C. Meyer, P. Birrer, G. Bellon, J. Berger, T. Weiss, K. Botzenhart, J. R. Yankaskas, S. Randell, R. C. Boucher and G. Döring, *J. Clin. Invest.*, 2002, **109**, 317-325.
8. A. S. Bayer, F. Eftekhar, J. Tu, C. C. Nast and D. P. Speert, *Infect. Immun.*, 1990, **58**, 1344-1349.
9. J. H. Leitão and Sá-Correia, *Res. Microbiol.*, 1997, **148**, 37-43.
10. D. W. Martin, B. W. Holloway and V. Deretic, *J. Bacteriol.*, 1993, **175**, 1153-1164.
11. C. D. Hershberger, R. W. Ye, M. R. Parsek, Z. D. Xie and A. M. Chakrabarty, *Proc. Natl. Acad. Sci. U. S. A.*, 1995, **92**, 7941-7945.
12. J. C. Boucher, M. J. Schurr and V. Deretic, *Mol. Microbiol.*, 2000, **36**, 341-351.
13. M. J. Schurr, H. Yu, J. M. Martinez-Salazar, J. C. Boucher and V. Deretic, *J. Bacteriol.*, 1996, **178**, 4997-5004.
14. J. C. Boucher, H. Yu, M. H. Mudd and V. Deretic, *Infect. Immun.*, 1997, **65**, 3838-3846.
15. D. W. Rowen and V. Deretic, *Mol. Microbiol.*, 2000, **36**, 314-327.
16. J. C. Boucher, M. J. Schurr, H. Yu, D. W. Rowen and V. Deretic, *Microbiology (Reading, U. K.)*, 1997, **143 (Pt 11)**, 3473-3480.
17. D. W. Martin, M. J. Schurr, M. H. Mudd, J. R. Govan, B. W. Holloway and V. Deretic, *Proc. Natl. Acad. Sci. U. S. A.*, 1993, **90**, 8377-8381.
18. A. M. Firoved, J. C. Boucher and V. Deretic, *J. Bacteriol.*, 2002, **184**, 1057-1064.
19. A. M. Firoved and V. Deretic, *J. Bacteriol.*, 2003, **185**, 1071-1081.
20. A. J. Carterson, L. A. Morici, D. W. Jackson, A. Frisk, S. E. Lizewski, R. Jupiter, K. Simpson, D. A. Kunz, S. H. Davis, J. R. Schurr, D. J. Hassett and M. J. Schurr, *J. Bacteriol.*, 2004, **186**, 6837-6844.
21. W. Wu, H. Badrane, S. Arora, H. V. Baker and S. Jin, *J. Bacteriol.*, 2004, **186**, 7575-7585.
22. C. B. Whitchurch, R. A. Alm and J. S. Mattick, *Proc. Natl. Acad. Sci. U. S. A.*, 1996, **93**, 9839-9843.
23. D. B. Kell and S. G. Oliver, *Bioessays*, 2004, **26**, 99-105.
24. D. J. Glass and N. Hall, *Cell*, 2008, **134**, 378-381.
25. L. Raamsdonk, B. Teusink, D. Broadhurst, N. Zhang, A. Hayes, M. Walsh, J. Berden, K. Brindle, D. Kell, J. Rowland, H. Westerhoff, K. van Dam and S. Oliver, *Nat. Biotechnol.*, 2001, **19**, 45-50.
26. J. G. Bundy, B. Papp, R. Harmston, R. A. Browne, E. M. Clayson, N. Burton, R. J. Reece, S. G. Oliver and K. M. Brindle, *Genome Res.*, 2007, **17**, 510-519.
27. S. G. Oliver, M. K. Winson, D. B. Kell and F. Baganz, *Trends Biotechnol.*, 1998, **16**, 373-378.
28. D. Ryan and K. Robards, *Anal. Chem.*, 2006, **78**, 7954-7958.
29. M. Oldiges, S. Lütz, S. Pflug, K. Schroer, N. Stein and C. Wiendahl, *Appl. Microbiol. Biotechnol.*, 2007, **76**, 495-511.
30. J. Allen, H. Davey, D. Broadhurst, J. Heald, J. Rowland, S. Oliver and D. Kell, *Nat. Biotechnol.*, 2003, **21**, 692-696.
31. N. N. Kaderbhai, D. I. Broadhurst, D. I. Ellis, R. Goodacre and D. B. Kell, *Comp. Funct. Genomics*, 2003, **4**, 376-391.

32. V. Behrends, T. M. D. Ebbels, H. D. Williams and J. G. Bundy, *Appl. Environ. Microbiol.,* 2009, **75**, 2453-2463.
33. K. L. Palmer, L. M. Aye and M. Whiteley, *J. Bacteriol.*, 2007, **189**, 8079-8087.
34. J. A. Fyfe and J. R. Govan, *J. Gen. Microbiol.*, 1980, **119**, 443-450.
35. J. Quandt and M. F. Hynes, *Gene*, 1993, **127**, 15-21.
36. O. Beckonert, H. C. Keun, T. M. D. Ebbels, J. Bundy, E. Holmes, J. C. Lindon and J. K. Nicholson, *Nat. Protoc.*, 2007, **2**, 2692-2703.
37. J. Trygg and S. Wold, *J. Chemom.*, 2002, **16**, 119-128.
38. O. Cloarec, M. E. Dumas, J. Trygg, A. Craig, R. H. Barton, J. C. Lindon, J. K. Nicholson and E. Holmes, *Anal. Chem.*, 2005, **77**, 517-526.
39. S. Wold, N. Kettaneh and K. Tjessem, *J. Chemom.*, 1996, **10**, 463-482.
40. M. R. D'Souza-Ault, L. T. Smith and G. M. Smith, *Appl. Environ. Microbiol.*, 1993, **59**, 473-478.
41. R. Velasco-García, M. A. Villalobos, M. A. Ramírez-Romero, C. Mújica-Jiménez, G. Iturriaga and R. A. Muñoz-Clares, *Arch. Microbiol.*, 2006, **185**, 14-22.
42. L. T. Smith and G. M. Smith, *J. Bacteriol.*, 1989, **171**, 4714-4717.
43. J. G. Bundy, T. L. Willey, R. S. Castell, D. J. Ellar and K. M. Brindle, *FEMS Microbiol. Lett.*, 2005, **242**, 127-136.
44. L. M. Keith and C. L. Bender, *J. Bacteriol.*, 1999, **181**, 7176-7184.
45. U. Schnider-Keel, K. B. Lejbølle, E. Baehler, D. Haas and C. Keel, *Appl. Environ. Microbiol.*, 2001, **67**, 5683-5693.
46. D. Qiu, V. M. Eisinger, D. W. Rowen and H. D. Yu, *Proc. Natl. Acad. Sci. U. S. A.*, 2007, **104**, 8107-8112.
47. P. J. Tatnell, N. J. Russell and P. Gacesa, *J. Gen. Microbiol.*, 1993, **139**, 119-127.
48. A. Berry, J. D. DeVault and A. M. Chakrabarty, *J. Bacteriol.*, 1989, **171**, 2312-2317.
49. A. Aspedon, K. Palmer and M. Whiteley, *J. Bacteriol.*, 2006, **188**, 2721-2725.
50. A. Farewell, K. Kvint and T. Nyström, *Mol. Microbiol.*, 1998, **29**, 1039-1051.
51. S. J. Suh, L. Silo-Suh, D. E. Woods, D. J. Hassett, S. E. West and D. E. Ohman, *J. Bacteriol.*, 1999, **181**, 3890-3897.
52. T. Nyström, *Mol. Microbiol.*, 2004, **54**, 855-862.
53. S. Kayama, K. Murakami, T. Ono, M. Ushimaru, A. Yamamoto, K. Hirota and Y. Miyake, *FEMS Microbiol. Lett.*, 2009, **298**, 184-192.
54. J. J. Smith, S. M. Travis, E. P. Greenberg and M. J. Welsh, *Cell*, 1996, **85**, 229-236.
55. T. W. Fan, T. D. Colmer, A. N. Lane and R. M. Higashi, *Anal. Biochem.*, 1993, **214**, 260-271.
56. R. A. Ciulla and M. F. Roberts, *Biochim. Biophys. Acta*, 1999, **1427**, 193-204.
57. V. Tremaroli, M. L. Workentine, A. M. Weljie, H. J. Vogel, H. Ceri, C. Viti, E. Tatti, P. Zhang, A. P. Hynes, R. J. Turner and D. Zannoni, *Appl. Environ. Microbiol.*, 2009, **75**, 719-728.
58. J. M. Beale and J. L. Foster, *Biochemistry*, 1996, **35**, 4492-4501.

59. S. Jain, M. J. Franklin, H. Ertesvåg, S. Valla and D. E. Ohman, *Mol. Microbiol.*, 2003, **47**, 1123-1133.
60. H. Ertesvåg, F. Erlien, G. Skjåk-Braek, B. H. Rehm and S. Valla, *J. Bacteriol.*, 1998, **180**, 3779-3784.

Figure legends

Figure 1: orthogonal Partial Least Squares-Discriminant Analysis of NMR spectra of culture supernatants sampled at 24 h reveal different pool sizes of amino acids valine and methionine, osmo-protectant glycine-betaine, disaccharide trehalose as well as an unassigned doublet at 5.26 ppm. Upward pointing resonances were correlated with (found to have higher levels in) supernatants of the wild-type, downward pointing resonances with supernatants of the *mucA22* mutant. Peak colour signifies strength of correlation as indicated. Inset: Amplified spectral region between 5.14 and 5.32 ppm.

Figure 2: Relative metabolite concentration changes over the course of growth reveal differences between *P. aeruginosa* PA01 and its isogenic *mucA22* mutant. A: Valine, B: Methionine, C: Glycine-betaine, D: Trehalose, E: Unassigned doublet at 5.26 ppm, F: Choline. Solid lines: wild-type, dashed lines: *mucA22* mutant. Error bars represent S.E.M (n=3).

Figure 3: Growth in media with elevated salt concentrations reveals a deficit in osmotolerance in the *mucA22* stationary phase cultures. A: Growth curve in LB medium supplemented with 0.4M NaCl (0-24 h), B: Growth curve in unsupplemented LB medium (0-24 h), C: Optical densities of cultures after 24h of growth in LB supplemented with different NaCl concentrations (0-0.8M), D: Culture viability of stationary phase cultures after growth for 24 h. Colony forming units ($cfu*ml^{-1}$), levels are given relative to PA01. E: Distribution and variance of optical densities of 24 h stationary phase cultures for wild-type and *mucA* mutant cultures grown in LB with different NaCl concentrations, F: ^{1}H NMR spectra of the spectral region between 5.0 and 5.8 ppm depicting the resonances of the unknown compounds found in the medium of some independent replicates of the *mucA22* mutant after 24 h of growth. Solid lines: wild-type, dashed lines: *mucA22* mutant. Error bars represent S.E.M (n=3) for A-C, n=72 for box-plot in E.

Figure 4: NaCl-concentration dependence of relative concentrations of osmoresponsive compounds in *P. aeruginosa* cells. Metabolites were extracted and analysed by NMR, as described in Methods section, from 24 h stationary phase cultures. A: Correlation analysis showing which compounds accumulate in *P. aeruginosa* cells with rising NaCl concentration in the medium; Concentration dependence of relative intracellular levels of NAGGN (B), glutamate (C), glycine-betaine (D), and trehalose (E). The values were integrated manually from NMR spectra normalized to total spectral area.

Figure 5: Sigmoid fitting of relative concentration coupled with H-PCA analysis reveals potential mechanistic difference in osmotic tolerance between *P. aeruginosa* PA01 and *mucA22*. PA01 and *mucA22* were grown for 24 h in unsupplemented LB as well as LB supplemented with 0.4M NaCl and analysed by TReF. A: Scores plot of PCA using raw, mean-centred NMR data as input. B: 2nd level scores plot of H-PCA using fitted sigmoid parameters as inputs. Colours in A and B: Purple: PA01, LB; red: *mucA22*, LB; black: PA01, LB+0.4M NaCl; yellow: *mucA22*, LB+0.4M NaCl, C: Plot describing the uptake parameters (‘uptake plot’) of the indicated compounds for PA01 grown in unsupplemented LB; D: Uptake plot for PA01 grown in LB supplemented with 0.4M NaCl; E: Uptake plot for *mucA22* grown in unsupplemented LB; F: Uptake plot for *mucA22* grown in LB supplemented with 0.4M NaCl. All three biological replicates are shown.

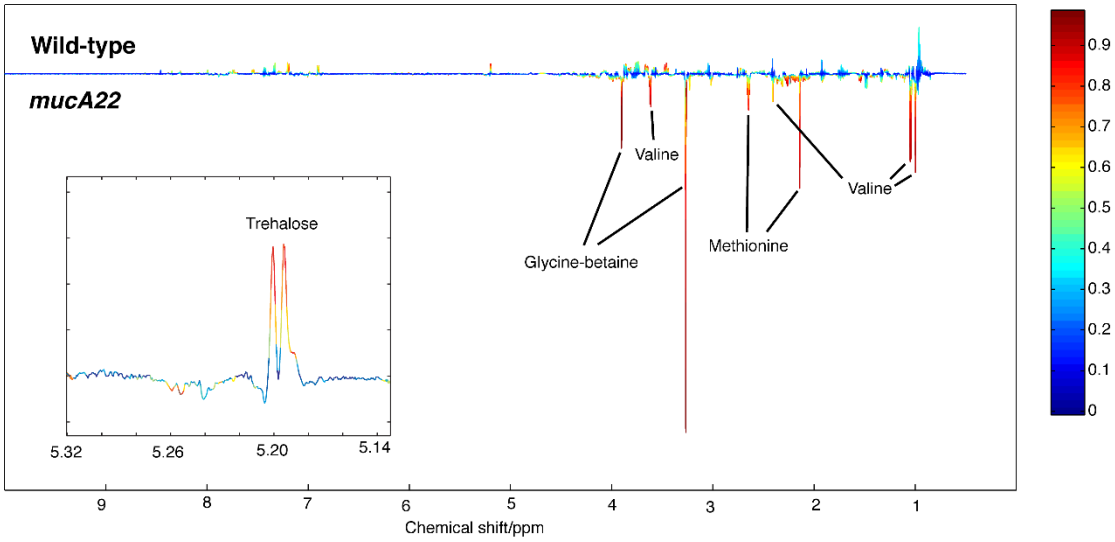
Wild-type
mucA22
Trehalose
5.32
5.26
5.20
5.14
Valine
Valine
Glycine-betaine
Methionine
9
8
7
6
5
4
3
2
1
Chemical shift/ppm
0.9
0.8
0.7
0.6
0.5
0.4
0.3
0.2
0.1
0

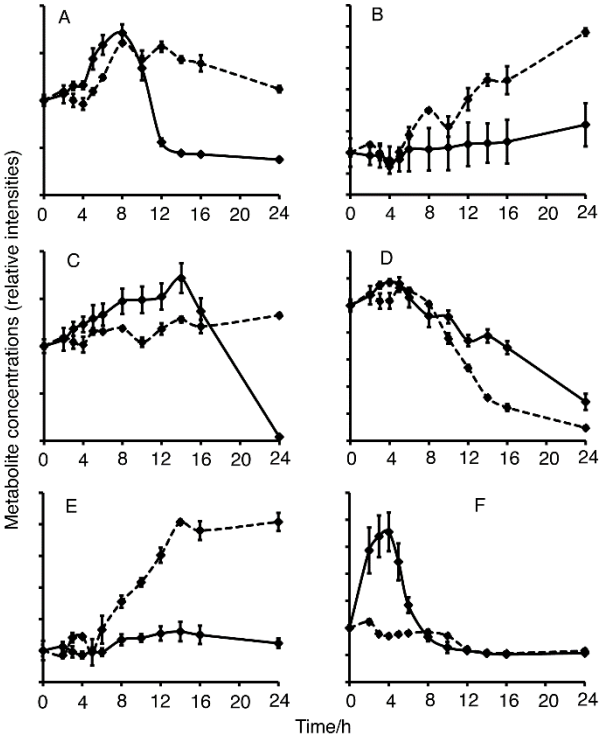
A
B
C
D
E
F
Metabolite concentrations (relative intensities)
0
4
8
12
16
20
24
Time/h

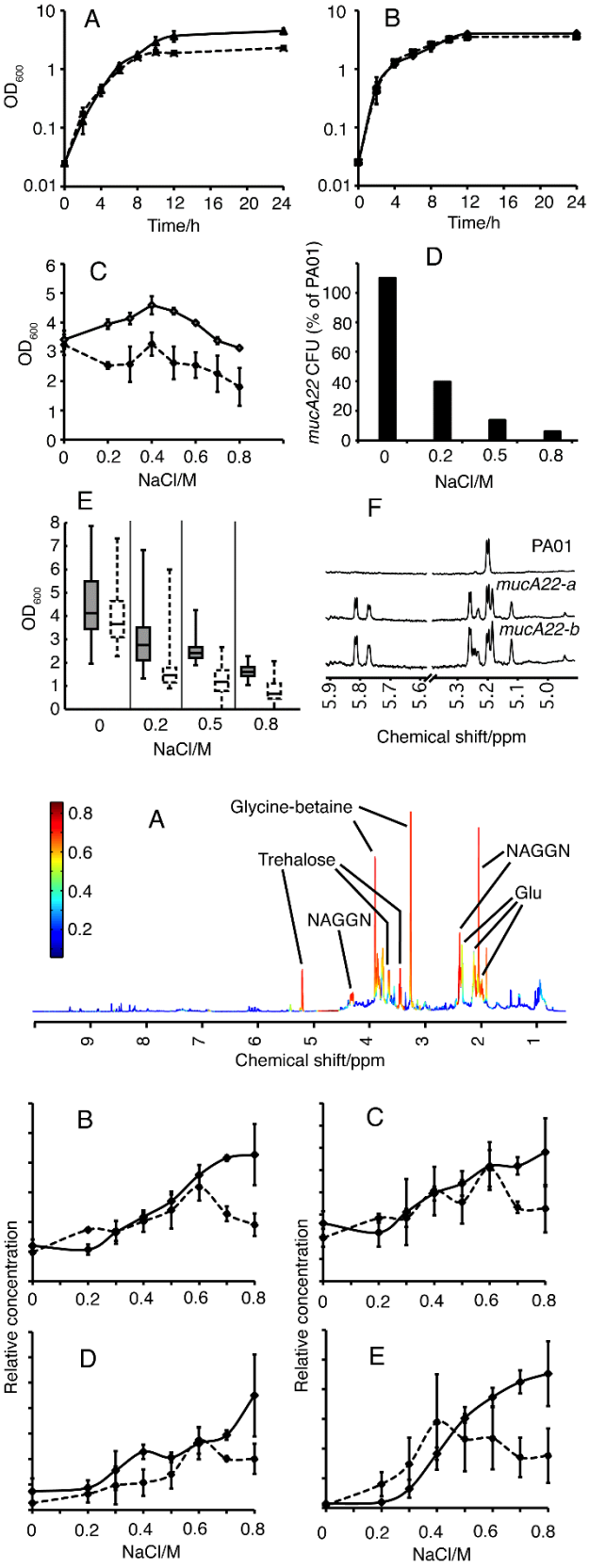
A
B
C
D
E
F
OD600
Time/h
NaCl/M
mucA22 CFU (% of PA01)
PA01
mucA22-a
mucA22-b
Chemical shift/ppm
Glycine-betaine
Trehalose
NAGGN
Glu
Relative concentration

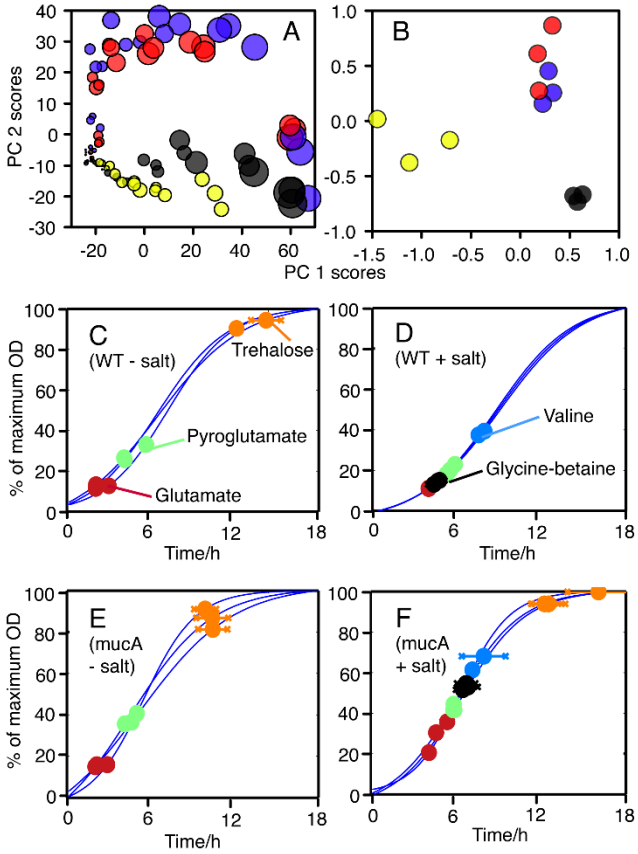
A
B
PC 2 scores
PC 1 scores
C
(WT - salt)
Trehalose
Pyroglutamate
Glutamate
D
(WT + salt)
Valine
Glycine-betaine
E
(mucA
- salt)
F
(mucA
+ salt)
% of maximum OD
Time/h